

Effect of tetrahydrofuran on the anionic copolymerization of 4-trimethylsilylstyrene with isoprene

Dominik A. H. Fuchs | Shivani P. Wadgaonkar | Axel H. E. Müller | Holger Frey 

Department of Chemistry, Johannes Gutenberg University, Mainz, Germany

Correspondence

Axel H. E. Müller and Holger Frey, Department of Chemistry, Johannes Gutenberg University, Duesbergweg 10-14, 55128 Mainz, Germany. Email: axel.mueller@uni-mainz.de; hfrey@uni-mainz.de

Abstract

The statistical anionic copolymerization of 4-trimethylsilylstyrene (TMSS) with isoprene (I) in cyclohexane was investigated using in situ near-infrared (NIR) spectroscopy in the presence of various amounts of the polar modifier tetrahydrofuran (THF). Polymers with narrow molecular weight distribution of 85–138 kg/mol and dispersities of 1.09–1.22 were obtained. By increasing modifier content, the reactivity ratios can be adjusted over a wide range from $r_{\text{TMSS}} < r_1$ to $r_{\text{TMSS}} \gg r_1$. Compared to the system styrene/isoprene (S/I) only a minute amount of modifier (0.5 eq THF relative to lithium) is sufficient to alter the reactivity ratios, resulting in an ideally random copolymerization, which validates the higher reactivity of TMSS compared to styrene. Using these reactivity ratios, molar and volume composition gradients were calculated. Additionally, the glass transition temperature and microstructure of the polyisoprene units were investigated via differential scanning calorimetry and proton nuclear magnetic resonance. The results are encouraging for the use of these materials in high-end applications like membranes.

KEYWORDS

anionic copolymerization, online monitoring, polyisoprene, reactivity ratio, styrene

1 | INTRODUCTION

Since the discovery of living anionic polymerization in 1956, both industry and research have been using this technique to produce polymers with tailored properties, in particular block copolymers and other high-performance materials.^{1–9} Most frequently, the products are based on styrene and diene monomers, which are polymerized under specific conditions to obtain nanophase-separated multiblock structures, which are used as thermoplastic elastomers.

In the copolymerization of styrene (S) with isoprene (I) in apolar solvents, such as cyclohexane, the diene polymerizes first until almost all diene monomer is consumed, as can be seen from the disparate

reactivity ratios: $r_S = 0.015$ and $r_I = 10.03$.¹⁰ This leads to a strong comonomer gradient along the chain and has been used to synthesize tapered block and multiblock copolymers.^{11,12} By adding only small amounts of polar modifiers (Lewis bases) like tetrahydrofuran (THF), these reactivity ratios can be drastically changed, leading to randomness or even inversion of reactivity ratios (2500 eq THF: $r_S = 12.58$ and $r_I = 0.012$).^{10,13} The addition of polar modifiers such as THF changes the polymerization kinetics, as the chain end is solvated differently and Li-related aggregation is reduced.^{10,14–16}

Besides styrene, different styrene derivatives can be used for the hard block, for instance, 4-trimethylsilylstyrene (4TMSS, in the following TMSS), which not only alters the reactivity ratios but also the gas permeation properties of the polymer.^{17,18} Yampolskii et al. showed that polytrimethylsilylstyrene (PTMSS) has a 1.4-fold higher free

Dedicated to Prof. Stanislaw Penczek on the occasion of his 90th birthday.

This is an open access article under the terms of the [Creative Commons Attribution](https://creativecommons.org/licenses/by/4.0/) License, which permits use, distribution and reproduction in any medium, provided the original work is properly cited.

© 2024 The Author(s). *Polymers for Advanced Technologies* published by John Wiley & Sons Ltd.

volume compared to polystyrene (PS) and shows a significant influence on the higher permeability compared to its carbon analog, poly(4-*tert*-butylstyrene).¹⁹ Nagasaki et al. proved that the C–Si linkage exhibits a strong affinity toward oxygen, which leads to an increase in the oxygen solubility coefficient.²⁰ Previous studies of the copolymerization of TMSS and isoprene using in situ proton nuclear magnetic resonance (¹H-NMR) kinetics revealed a less steep gradient structure ($r_1 = 3.28$; $r_{\text{TMSS}} = 0.152$).¹⁷ The introduction of the trimethylsilyl (TMS) group into the styrene monomer significantly increases its reactivity, and thus its reactivity ratio. The TMS group has an electron-donating (+I) and an electron-withdrawing (–M) effect when directly bound to an aromatic ring.^{21,22} These effects act in an opposite direction, and several studies suggest that the –M effect dominates when directly bound to the phenyl ring. Interaction of the empty 3d silicon orbitals with the π -orbitals of the phenyl ring leads to a downfield shift of the β -carbon and thus to a higher polarity and reactivity of TMSS.^{21,23,24} This increased reactivity compared to styrene could possibly be enhanced further by adding increasing amounts of THF to cyclohexane, which enables the synthesis of copolymers with various polymer compositions. For these studies, we used in situ near-infrared (NIR) spectroscopy, as described in our previous studies.^{10,14,25} The copolymers of TMSS and isoprene are investigated with respect to their polymer composition, microstructure, and thermal properties for possible application in gas separation membranes.

2 | EXPERIMENTAL SECTION

Materials, instrumentation, monomer synthesis, and copolymerization procedures are given in the [Supporting Information](#).

3 | RESULTS AND DISCUSSION

3.1 | Copolymerization kinetics

To investigate the effect of polar modifiers (THF) on the copolymerization of TMSS with isoprene, copolymerizations with different modifier content were performed in cyclohexane at 20°C with

sec-butyllithium (BuLi) as an initiator, similar to our previous studies.^{10,14} A molar ratio of 70 mol% of isoprene (density $\rho_{\text{PI}} = 0.91\text{g/L}$)²⁶ and 30 mol% of TMSS ($\rho_{\text{PTMSS}} = 0.963\text{g/L}$)²⁷ was used for the copolymerization to obtain polymers with 47.3 wt% and 48.8 vol% of isoprene, respectively. The size exclusion chromatography (SEC) elugrams of the copolymers (Figure S1) show that we obtained polymers with M_n between 85 and 138 kg/mol with dispersities between 1.09 and 1.22 (Table 1). Higher molecular weights can be explained by the approx. 10% overestimation of the polyisoprene (PI) samples when using a PS calibration.(ste). Some elugrams show a small peak or shoulder at lower elution volume stemming from oxygen coupling due to insufficient degassing of the termination reagent isopropanol.⁸

During the copolymerization, 13,000 to 20,000 NIR spectra in the range of 5900–6250 cm^{-1} were recorded and analyzed by deconvoluting the measured spectra with the calibration spectra of all components present (TMSS, PTMSS, and isoprene), as shown in Figure S2. Since the NIR spectrum of PI depends on its microstructure (given by the THF content), it was obtained by subtracting the spectra of the other components from the spectrum taken at full conversion. Plots of time vs conversion and of individual vs total conversion are given for 0.25 eq THF in Figure 1 and in the [Supporting Information](#) in Figures S3 and S4. It is clearly seen that with increasing content of THF, the rate of TMSS consumption strongly increases, whereas the rate of isoprene conversion is much less affected.

The reactivity ratios r_{TMSS} and r_1 were calculated using both the terminal and non-terminal models. The non-terminal model assumes an ideal copolymerization ($r_1 \cdot r_2 = 1$). If the plot according to Jaacks^{28,29} is linear, this model is assumed to be valid, thus avoiding overfitting. A numerical fit to a plot according to Meyer and Lowry³⁰ is used to calculate r_1 and r_2 independently is only necessary to fit the copolymerization in pure cyclohexane.^{31,32} The individual fits of the different methods can be seen in Figures S5 and S6.

Our results in pure cyclohexane are in reasonable agreement with values determined by Wadgaonkar et al. at room temperature with in situ ¹H-NMR ($r_{\text{TMSS}} = 0.152$ and $r_1 = 3.28$),¹⁷ The slight differences can be explained by different reaction temperatures, concentrations, deuterated solvents, and slow diffusion in an NMR tube.

Table 1 and Figure 2 show the strong effect of THF on the reactivity ratios, particularly on r_{TMSS} . This is similar to earlier observations

TABLE 1 Effect of THF on the reactivity ratios, molecular weight, dispersity, and blockiness for P(TMSS_{0.3}-co-I_{0.7}). Initiator and total monomer concentrations are 1.75 mmol/L and 1.4 mol/L, respectively.

[THF]/[Li]	Φ_{THF} , %Vol	ϵ^a	r_{TMSS}	r_1	$r_{\text{TMSS}} \times r_1$	Blockiness	M_n^b (kg/mol)	\mathcal{D}^b
0	0	2.023	0.066	2.37	0.16	37.7	84.6	1.15
0.25	0.0035	2.023	0.74	1.36	1	7.2	138.4	1.12
0.5	0.007	2.024	1.09	0.92	1	2.1	99.2	1.22
2	0.028	2.026	2.04	0.49	1	3.4	122.2	1.09
20	0.28	2.049	4.52	0.22	1	16.1	121.5	1.11
200	2.85	2.268	22.9	0.04	1	68.6	121.3	1.14

^aDielectric constant of solvent.

^bsize exclusion Chromatography (SEC) calibration with PS standards.

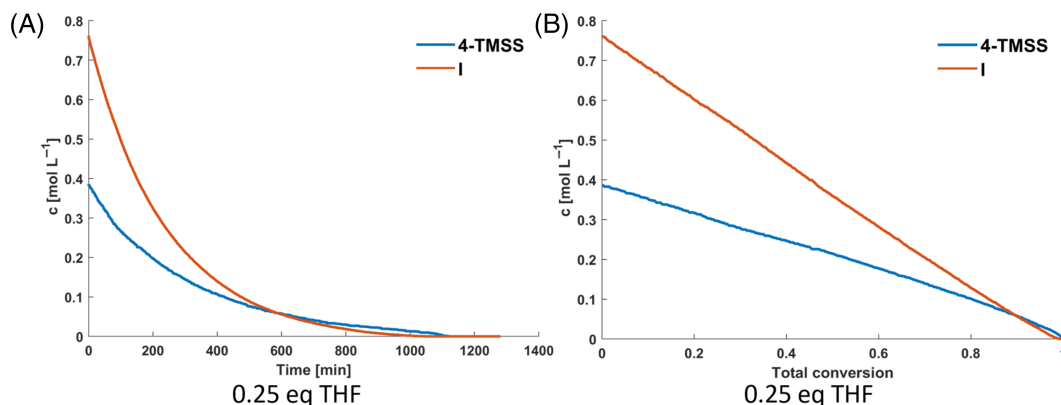


FIGURE 1 (A) Time conversion plot and (B) monomer concentration as a function of total conversion for $[\text{THF}]/[\text{Li}] = 0.25$.

in the systems S/I and S/myrcene. Already at a ratio $\text{THF}/\text{Li} \approx 0.4$ randomization is observed (Table S1). In contrast, a ratio $\text{THF}/\text{Li} \approx 6$ is required to reach the formation of ideally random copolymers in the S/I system. Thus, TMSS is considerably more sensitive to polar modifiers than styrene. This is explained by the higher reactivity of TMSS, caused by the electron-withdrawing effect of the trimethylsilyl group, as described earlier.¹⁷

3.2 | Shape of the gradient

The obtained reactivity ratios were used to calculate the gradients of comonomer compositions, Figure 3A shows the molar fraction of TMSS units, F_{TMSS} , as a function of total conversion (i.e., along the polymer chain) and Figure 3B shows the volume incorporation, $F_{\text{TMSS},V}$, along the chain.

The copolymerization without modifier yields a tapered copolymer that initially forms an isoprene block interspersed with short TMSS segments and, after all isoprene has been consumed, a pure PTMSS block is formed. Increasing the modifier content changes the composition: As the modifier content increases up to 0.5 eq, the gradient flattens out and almost random copolymers are obtained. Increasing the THF content further the gradient steepens again, and for ≥ 20 eq., a PTMSS block with short PI segments is formed and only after TMSS has been completely consumed is a pure PI block formed.

In addition, the so-called “blockiness” was determined by analyzing the $^1\text{H-NMR}$ spectra of the copolymers in Figure 4.^{33–36} The values are presented in Table 1 and confirm the kinetically obtained gradients. Details are given in the Supporting Information.

3.3 | Microstructure of isoprene units

$^1\text{H-NMR}$ spectroscopy was used to determine the microstructure of the isoprene monomer units. This method differs from the one previously used by us consisting of a combination of inverse-gated ^{13}C NMR and ^1H NMR.¹⁰ In contrast to the evaluation of the S/I system, for our monomer combination, there is a significant overlap of the h and n signals (see Figures S10–S15). A comparison of the two

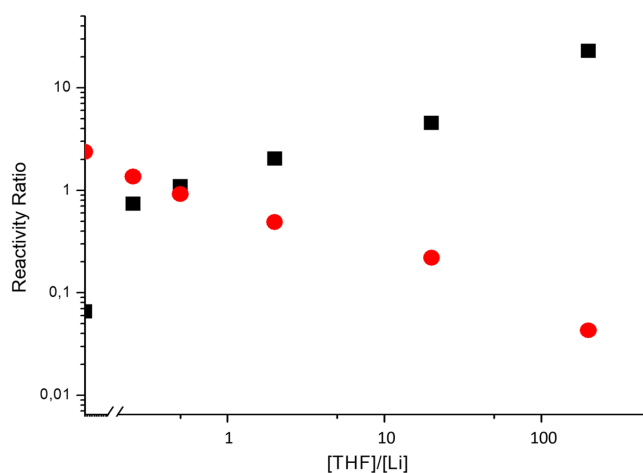


FIGURE 2 Reactivity ratios of r_{TMSS} (black squares) and r_I (red circles) in dependence on the THF modifier content.

methods shows minor differences at lower 1,4-contents.¹⁰ $^1\text{H-}$, $^{13}\text{C}_{\text{ig-}}$, COSY, HSQC, and heteronuclear multiple bond correlation spectra of the copolymers, and the exact calculation can be found in Figures S7–S16. An overview of the $^1\text{H-NMR}$ spectra is shown in Figure 4, and the PI microstructure is listed in Table 2.

When synthesized in pure cyclohexane, the isoprene units consist of 6% 3,4- and 94% 1,4-units, which is in good agreement with the literature.^{10,25,37,38} With increasing modifier concentration the 1,4- content decreases, and the 3,4- and 1,2- amount increases (Figure 5). For $\text{THF}/\text{Li} \geq 0.5$, 1,2-units appear, as shown in the green areas in Figure 4. Taking into account the different analytical methods, these results agree well with the literature. In addition, different concentrations of monomers, chain ends, and increased polarity due to the TMSS comonomer may have an impact on the results.^{10,39,40}

3.4 | Thermal properties

The thermal properties of the copolymers were investigated by differential scanning calorimetry (DSC), and the results are shown in Table 2 and Figure 6. The DSC curves are shown in Figure S17. For all

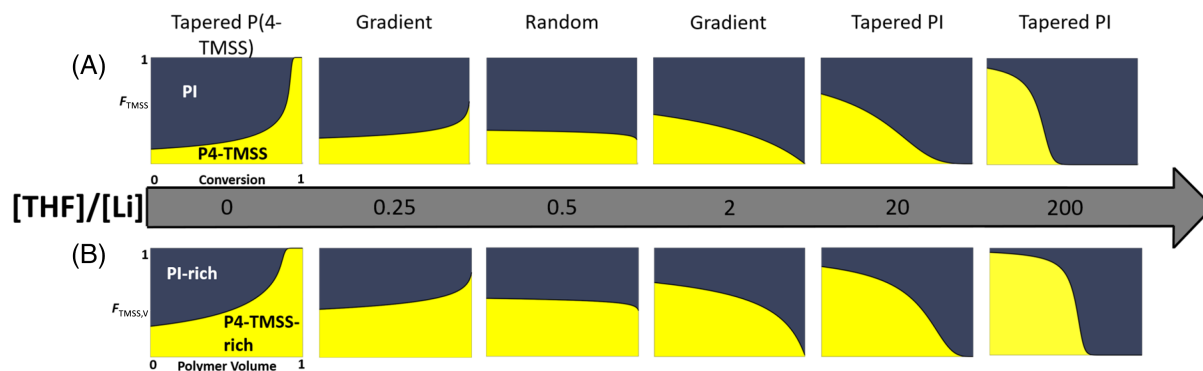


FIGURE 3 (A) Molar (B) volume composition of the P(TMSS_{0.3}-co-I_{0.7}) copolymer as a function of the [THF]/[Li] ratio.

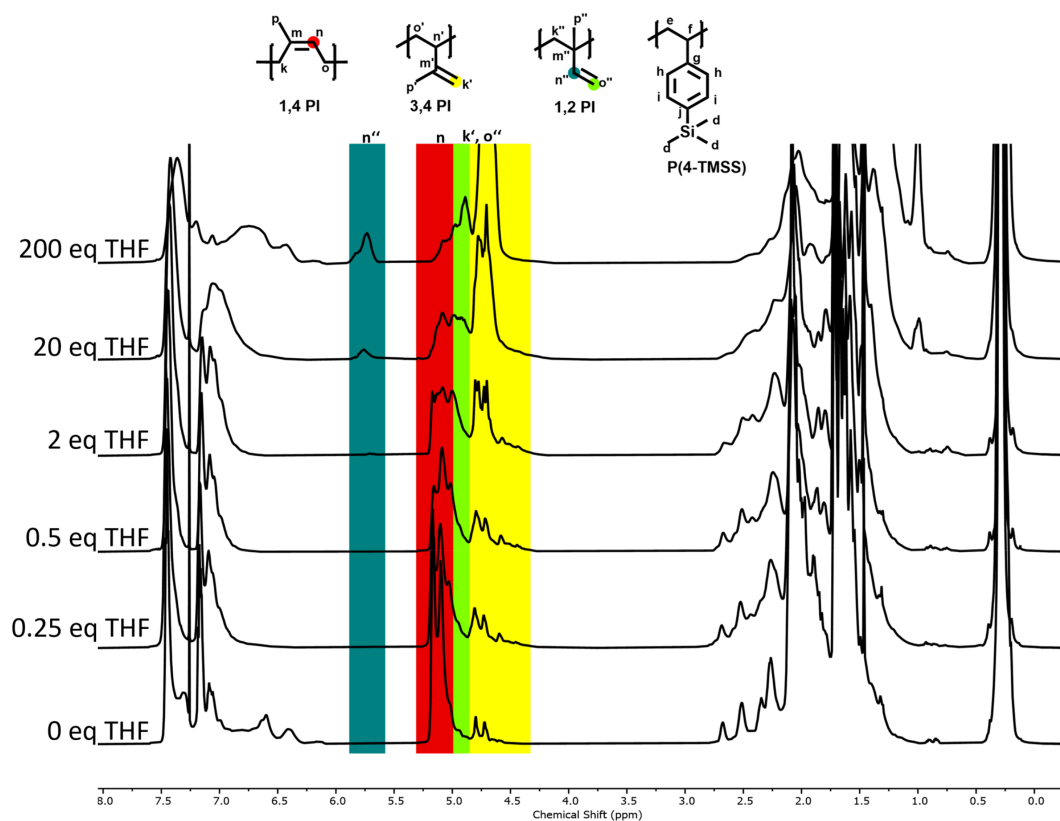


FIGURE 4 Overview of all ¹H-NMR spectra (CDCl₃, 600 MHz) of P(TMSS-co-I) prepared in cyclohexane with 0 ≤ [THF]/[Li] ≤ 200.

TABLE 2 Microstructure of isoprene monomer units in P(TMSS_{0.3}-co-I_{0.7}) determined by ¹H-NMR spectroscopy, the inherent glass transition temperatures (T_g), and the temperature at 5% wt. loss (determined by thermogravimetric analysis), considered as the onset of thermal decomposition.

[THF]/[Li]	1,4-PI (%)	3,4-PI (%)	1,2-PI (%)	T_g (°C)	$T_{5\%}$ (°C)
0	93.7	6.3	0	-22	348
0.25	85	15	0	5	328
0.5	80.3	18.6	1.1	8	350
2	69.0	28.6	2.4	16	342
20	40.8	52.2	7.0	30	345
200	16.7	66.7	16.6	36	336

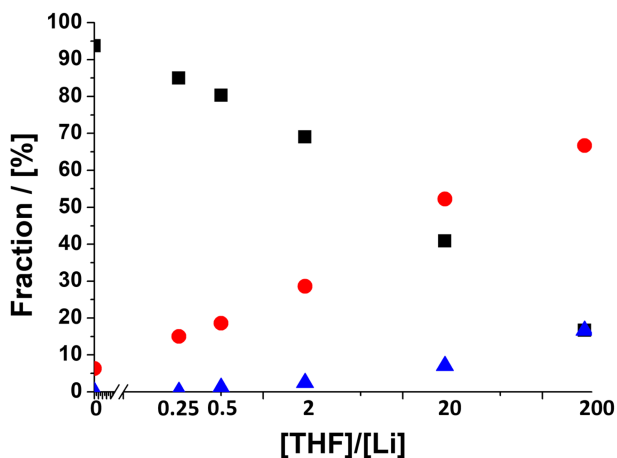


FIGURE 5 Microstructure of the isoprene units (1,4-black squares; 3,4-red dots; 1,2-blue triangle) as a function of the ratio $[THF]/[Li]$ for the copolymer $P(TMSS_{0.3-co-I_{0.7}}$.

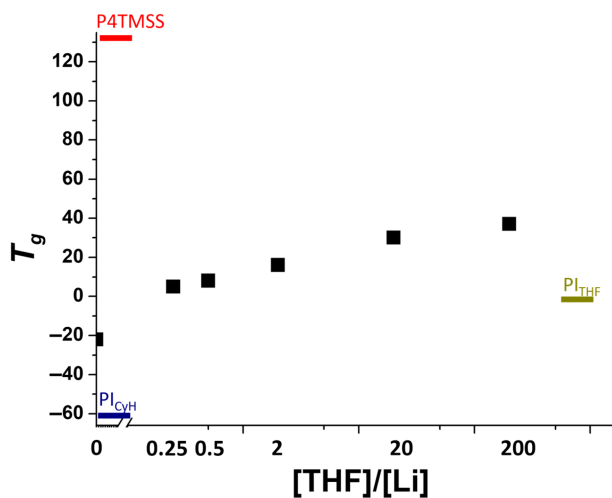


FIGURE 6 Glass transition temperature of the copolymer $P(TMSS_{0.3-co-I_{0.7}}$, as a function of the $[THF]/[Li]$ ratio. The horizontal lines symbolize the glass transition temperature of the homopolymers PTMSS and PI synthesized in cyclohexane and THF.

samples, only a single glass transition temperature was measured, despite the high molecular weights of the materials in the range of 80–138 kg/mol, indicating that no phase separation takes place. In our earlier paper, this was also observed for the gradient copolymer synthesized in pure cyclohexane. In contrast, the block copolymer $P(I_{0.5-b-TMSS_{0.5}}$, synthesized by sequential monomer additions, has two distinct glass transition temperatures (-49.9°C and 53.8°C).¹⁷ They strongly differ from the respective homopolymers and suggest partial mixing of both phases, which indicates that the Flory-Huggins parameter, $\chi_{TMSS/1,4-PI}$, is very small. Thus, it might be expected that a gradient-copolymer is not phase-separated, even for a rather strong gradient.

For 0 eq THF, the glass transition was measured at -22°C which is in good agreement with literature and is explained by a mixture of

both T_g , since both phases are miscible.¹⁷ PI synthesized in cyclohexane has $T_g = -64^\circ\text{C}$ ³⁸ and PTMSS has $T_g = 135^\circ\text{C}$.^{17,41}

THF affects the microstructure of the PI units and thus the glass transition temperature of the copolymers.^{42–45} As expected, with increasing modifier content, the glass transition temperature of this copolymer also increases.

From the similar system S/I it is known that the Flory-Huggins parameter, $\chi_{PS/PI}$, differs for the different PI microstructures.⁴⁶ Using the Hildebrand solubility parameters we estimated $\chi_{TMSS/1,4-PI} \approx 0.01$ and $\chi_{TMSS/3,4-PI} \approx 0$.¹⁷ Since 3,4-PI is the predominant microstructure when synthesized in the presence of 200 eq THF no phase separation can be expected. All mixed-phase polymers form stable films by solvent casting (Figure S18). In addition, all samples were analyzed by thermogravimetric analysis under nitrogen to investigate their thermostability. All samples showed a similar degradation temperature ($T_{5\%}$) of $330\text{--}350^\circ\text{C}$, at which a loss of 5 wt% occurred (see Table 2 and Figure S19); this is in the range of the homopolymers P(TMSS): 320°C ⁴⁷ and PI: 393°C .³ All polymers showed a one-step degradation and a complete decomposition at about 500°C .

4 | CONCLUSIONS

The kinetics of the copolymerization of TMSS with isoprene in the presence of different THF contents was successfully investigated by in situ NIR spectroscopy. The monomer TMSS shows a higher reactivity than styrene; already less than 0.5 equivalents of the polar modifier THF relative to Li^+ are sufficient to alter the reactivity ratios from a strong gradient into a random copolymerization. With increased modifier content the reactivity ratios are inverted leading to almost blocklike structures. The absence of two glass transition temperatures indicates the absence of phase separation. These polymers are potential candidates for gas separation membranes. The 3,4- and 1,2-monomer units of isoprene can be used for potential crosslinking reactions to form a stable 3D network.

ACKNOWLEDGMENTS

Dominik A. H. Fuchs thanks Jirui Zhang for helpful discussions, NMR analysis, and critical evaluation of this article. Open Access funding enabled and organized by Projekt DEAL.

CONFLICT OF INTEREST STATEMENT

There are no conflicts to declare.

DATA AVAILABILITY STATEMENT

The data that support the findings of this study are available from the corresponding author upon reasonable request.

ORCID

Holger Frey  <https://orcid.org/0000-0002-9916-3103>

REFERENCES

1. Szwarc M. 'Living' polymers. *Nature*. 1956;178:1168-1169.

2. Meier-Merziger M, Fickenscher M, Hartmann F, et al. Synthesis of phase-separated super-H-shaped triblock architectures: poly(l-lactide) grafted from telechelic polyisoprene. *Polym Chem*. 2023;14:2820-2828.
3. Zhang J, Pointer W, Patias G, et al. End functionalization of polyisoprene and polymyrcene obtained by anionic polymerization via one-pot ring-opening mono-addition of epoxides. *Eur Polym J*. 2023;183:111755.
4. Kim H, Goseki R, Homma C, Ishizone T. Synthesis of sequence-controlled homopolymer via anionic self-alternating and chemoselective polymerization of 4-Vinyl-1,1-diphenylethylene derivatives. *Macromolecules*. 2023;56:8796-8805.
5. Glatzel J, Noack S, Schanzenbach D, Schlaad H. Anionic polymerization of dienes in 'green' solvents. *Polym Int*. 2021;70:181-184.
6. Dev A, Rösler A, Schlaad H. Limonene as a renewable unsaturated hydrocarbon solvent for living anionic polymerization of β -myrcene. *Polym Chem*. 2021;12:3084-3087.
7. Ntetsikas K, Ladelta V, Bhaumik S, Hadjichristidis N. Quo Vadis carbanionic polymerization? *ACS Polym Au*. 2023;3:158-181.
8. Steube M, Johann T, Barent RD, Müller AHE, Frey H. Rational design of tapered multiblock copolymers for thermoplastic elastomers. *Prog Polym Sci*. 2022;124:101488.
9. Dong R, Gao A, Zhu Y, Xu B, Du J, Ping S. The development of a new thermoplastic elastomer (TPE)-modified asphalt. *Buildings*. 2023;13:1451.
10. Steube M, Johann T, Hübner H, et al. Tetrahydrofuran: more than a "randomizer" in the living anionic copolymerization of styrene and isoprene: kinetics, microstructures, morphologies, and mechanical properties. *Macromolecules*. 2020;53:5512-5527.
11. Porter R. Milkovich, Phillips Petroleum Co, GB888624A *Block Polymers and Process for Preparation Thereof*, 1959.
12. Holden G, Milkovich R. Block Polymers of Monovinyl Aromatic Hydrocarbons and Conjugated Dienes, U.S. Patent 3265765, 1962.
13. Shaw L, Hutchings LR. Tales of the unexpected. The non-random statistical copolymerisation of myrcene and styrene in the presence of a polar modifier. *Polym Chem*. 2020;11:7020-7025.
14. Fuchs DAH, Hübner H, Kraus T, et al. The effect of THF and the chelating modifier DTHFP on the copolymerisation of β -myrcene and styrene: kinetics, microstructures, morphologies, and mechanical properties. *Polym Chem*. 2021;12:4632-4642.
15. Morton M, Fetters LJ. Homogeneous anionic polymerization. V. Association phenomena in organolithium polymerization. *J Polym Sci A*. 1964;2:3311-3326.
16. Bywater S, Worsfold DJ. Anionic polymerization of styrene effect of tetrahydrofuran. *Can J Chem*. 1962;40:1564-1570.
17. Wadgaonkar SP, Schüttner S, Berger-Nicoletti E, Müller AHE, Frey H. Anionic copolymerization of 4-trimethylsilylstyrene: from kinetics to gradient and block copolymers. *Macromolecules*. 2022;55:4721-4732.
18. Khotimskii VS, Filippova VG, Bryantseva IS, Bondar VI, Shantarovich VP, Yampolskii YP. Synthesis, transport, and sorption properties and free volume of polystyrene derivatives containing Si and F. *J Appl Polym Sci*. 2000;78:1612-1620.
19. Puleo AC, Muruganandam N, Paul DR. Gas sorption and transport in substituted polystyrenes. *J Polym Sci B*. 1989;27:2385-2406.
20. Nagasaki Y, Hashimoto Y, Kato M, Kimijima T. Gas permeation properties of organosilicon-containing polystyrenes. *J Membr Sci*. 1996;110:91-97.
21. Vignollet Y, Maire JC, Witanowski M. Interaction between a phenyl ring and silicon atom. The nitrogen-14 nuclear magnetic resonance of nitrophenyltrimethylsilanes. *Chem Commun (London)*. 1968;0:1187.
22. Freedman LD, Tauber H, Doak GO, Magnuson HJ. The preparation of some organophosphorus compounds possessing anticholinesterase Activity1. *J Am Chem Soc*. 1953;75:1379-1381.
23. Ishizone T, Hirao A, Nakahama S. Anionic polymerization of monomers containing functional groups. 6. Anionic block copolymerization of styrene derivatives para-substituted with electron-withdrawing groups. *Macromolecules*. 1993;26:6964-6975.
24. Nagy J, Réffy J. Quantum chemical calculations of saturated, unsaturated, and aromatic compounds of silicon I. The calculation of σ - π interaction and σ bond systems. *J Organomet Chem*. 1970;22:565-572.
25. Steube M, Johann T, Plank M, et al. Kinetics of Anionic living copolymerization of isoprene and styrene using in situ NIR spectroscopy: temperature effects on monomer sequence and morphology. *Macromolecules*. 2019;52:9299-9310.
26. Mark JE. *Polymer Data Handbook*. Wiley; 1999.
27. Cushen JD, Wan L, Pandav G, et al. Ordering poly(trimethylsilyl styrene-block-D,L-lactide) block copolymers in thin films by solvent annealing using a mixture of domain-selective solvents. *J Polym Sci B*. 2014;52:36-45.
28. Jaacks V. Eine neuartige Methode zur Bestimmung von Copolymerisationsparametern. *Angew Chem*. 1967;79:419.
29. Jaacks V. A novel method of determination of reactivity ratios in binary and ternary copolymerizations. *Makromol Chem*. 1972;161:161-172.
30. Meyer VE, Lowry GG. Integral and differential binary copolymerization equations. *J Polym Sci A*. 1965;3:2843-2851.
31. Kazemi N, Duever TA, Penlidis A. Reactivity ratio estimation from cumulative copolymer composition data. *Macromol React Eng*. 2011;5:385-403.
32. Hautus FLM, German AL, Linssen HN. On numerical problems when reactivity ratios are computed using the integrated copolymer equation. *J Polym Sci: Polym Lett*. 1985;23:311-315.
33. Sardelis K, Michels HJ, Allen G, FRS. Graded block and randomized copolymers of butadiene-styrene. *Polymer (Guildf)*. 1984;25:1011-1019.
34. Mochel VD. NMR composition analysis of copolymers. *Rubber Chem Technol*. 1967;40:1200-1211.
35. Hogan TE, Kiridena W, Kocsis L. Effect of stereochemistry in anionic polymerization modifiers. *Rubber Chem Technol*. 2017;90:325-336.
36. Handlin DL. Block Copolymer US 6,699,941 B1 to Kraton Polymers U.S. LLC, 2004.
37. Wahlen C, Blankenburg J, Von Tiedemann P, et al. Tapered multiblock copolymers based on Farnesene and styrene: impact of biobased polydiene architectures on material properties. *Macromolecules*. 2020;53:10397-10408.
38. Worsfold DJ, Bywater S. Anionic polymerization of isoprene. *Can J Chem*. 1964;42:2884-2892.
39. Antkowiak TA, Oberster AE, Halasa AF, Tate DP. Temperature and concentration effects on polar modified alkyllithium polymerizations and copolymerizations. *J Polym Sci A*. 1972;10(5):1319-1334.
40. Uraneck CA. Influence of temperature on microstructure of anionic-initiated polybutadiene. *J Polym Sci A1*. 1971;9(8):2273-2281.
41. Kawakami Y, Karasawa H, Aoki T, Yamamura Y, Hisada H, Yamashita Y. Polymers with oligoorganosiloxane side chains as material for oxygen permeable membranes. *Polym J*. 1985;17:1159-1172.
42. Widmaier JM, Meyer GC. Glass transition temperature of anionic polyisoprene. *Macromolecules*. 1981;14:450-452.
43. Rüttiger C, Appold M, Didzoleit H, et al. Structure formation of metallopolymer-grafted block copolymers. *Macromolecules*. 2016;49:3415-3426.
44. Zhang L, Luo Y, Hou Z. Unprecedented isospecific 3,4-polymerization of isoprene by cationic rare earth metal alkyl species resulting from a binuclear precursor. *J Am Chem Soc*. 2005;127:14562-14563.
45. Jia X, Zhang X, Gong D. 1,2 Enriched polymerization of isoprene by cobalt complex carrying aminophosphory fused (PN3) ligand. *J Polym Sci A: Polym Chem*. 2018;56:2286-2293.
46. Owens JN, Gancarz IS, Koberstein JT, Russell TP. Investigation of the microphase separation transition in low-molecular-weight diblock copolymers. *Macromolecules*. 1989;22:3380-3387.

47. Cushen JD, Bates CM, Rausch EL, et al. Thin film self-assembly of poly(trimethylsilylstyrene-*b*-D,L-lactide) with sub-10 nm domains. *Macromolecules*. 2012;45:8722-8728.

SUPPORTING INFORMATION

Additional supporting information can be found online in the Supporting Information section at the end of this article.

How to cite this article: Fuchs DAH, Wadgaonkar SP, Müller AHE, Frey H. Effect of tetrahydrofuran on the anionic copolymerization of 4-trimethylsilylstyrene with isoprene. *Polym Adv Technol*. 2024;35(6):e6478. doi:[10.1002/pat.6478](https://doi.org/10.1002/pat.6478)